

Possibility to study pentaquark states $P_c(4312)$, $P_c(4440)$, and $P_c(4457)$ in the reaction $\gamma p \rightarrow J/\psi p$

Xiao-Yun Wang,^{1,*} Xu-Rong Chen,^{2,†} and Jun He^{3,‡}

¹Department of physics, Lanzhou University of Technology, Lanzhou 730050, China

²Institute of Modern Physics, Chinese Academy of Sciences, Lanzhou 730000, China

³Department of Physics and Institute of Theoretical Physics,
Nanjing Normal University, Nanjing, Jiangsu 210097, China

Inspired by the observation of the pentaquark states $P_c(4312)$, $P_c(4440)$ and $P_c(4457)$ at LHCb, photoproduction of these three P_c states via the interaction $\gamma p \rightarrow J/\psi p$ is investigated in an effective Lagrangian approach. The t -channel Pomeron exchange diffractive process is considered as the main background for the J/ψ photoproduction. The numerical results show that the theoretical cross section, which is calculated by assuming a branching ratio $Br[P_c \rightarrow J/\psi p] \approx 3\%$, is consistent with the existing experimental data of the $\gamma p \rightarrow J/\psi p$ process. With such a branching ratio, if experimental precision reaches 0.1 nb within a bin of 100 MeV for photon energy, two peaks are expected to be obviously observed in the J/ψ photoproduction. To observe the two-peak structure from $P_c(4440)$ and $P_c(4457)$, higher precision, about 0.1nb/10 MeV, is required to distinguish two close pentaquarks. If the physical branching ratio is larger, the requirement of experimental precision will be reduced. The differential cross sections for reaction $\gamma p \rightarrow J/\psi p$ are also present. It is found that the t -channel Pomeron exchange provides a sharp increase at extreme forward angles and gives a sizable contribution at most energy points, while the contributions from the s -channel P_c exchanges play important roles at threshold energies. The experimental measurement of the $\gamma p \rightarrow J/\psi p$ process in the near-threshold energy region around $E_\gamma \approx 9.4 - 10.5$ GeV is suggested, and is accessible at CEBAF@JLab and COMPASS.

PACS numbers: 13.60.Rj, 11.10.Ef, 12.40.Vv, 12.39.Mk

I. INTRODUCTION

As of now, many exotic hadrons have been observed and listed in the Review of Particle Physics (PDG) [1]. However, the internal structure of these exotic hadrons is still a confusing problem. The pentaquark is a type of important exotic hadron. In 2015, LHCb reported their observation of two pentaquark candidates, $P_c(4450)$ and $P_c(4380)$ [2]. Very recently, an updated result was reported: three narrow pentaquark states, $P_c(4312)$, $P_c(4440)$, and $P_c(4457)$, were observed in the $J/\psi p$ invariant mass spectrum of the $\Lambda_b \rightarrow J/\psi p K$ decays [3]. It is interesting to see that the $P_c(4450)$ formerly reported by the LHCb Collaboration [2] splits into two peaks, $P_c(4440)$ and $P_c(4457)$, based on more accumulated data. The masses and widths of these three P_c states were measured [3]:

$$\begin{aligned}
 P_c^+(4312) : M &= 4311.9 \pm 0.7_{-0.6}^{+6.8} \text{ MeV}, \\
 \Gamma &= 9.8 \pm 2.7_{-4.5}^{+3.7} \text{ MeV}, \\
 P_c^+(4440) : M &= 4440.3 \pm 1.3_{-4.7}^{+4.1} \text{ MeV}, \\
 \Gamma &= 20.6 \pm 4.9_{-10.1}^{+8.7} \text{ MeV}, \\
 P_c^+(4457) : M &= 4457.3 \pm 0.6_{-1.7}^{+4.1} \text{ MeV}, \\
 \Gamma &= 6.4 \pm 2.0_{-1.9}^{+5.7} \text{ MeV}. \quad (1)
 \end{aligned}$$

The nature of these three P_c states attracts much attention and has been studied by many theoretical models [4–15]. Among these theoretical investigations, the spin parities of these P_c states were also predicted. It can be seen that these three P_c states are quite narrow and can be clearly seen in

the $J/\psi p$ invariant mass spectrum. Moreover, closeness of the $\Sigma_c \bar{D}$ or $\Sigma_c \bar{D}^*$ thresholds to these three structures suggests that the $\Sigma_c \bar{D}$ and $\Sigma_c \bar{D}^*$ interactions play important roles in the dynamics of these P_c states. Accordingly, one notices that many of theoretical studies suggested that the $P_c(4312)$ can be assigned as an S-wave $\Sigma_c \bar{D}$ bound state with spin parity $1/2^-$ and the $P_c(4440)$ and $P_c(4457)$ as S-wave $\Sigma_c \bar{D}^*$ bound states with spin parities $1/2^-$ and $3/2^-$, respectively [4, 6–8, 10, 13]. At the hadronic level, the P_c states as molecular states are generated from the $\Sigma^{(*)} \bar{D}^{(*)}$ interaction in the one-boson-exchange model in which pseudoscalar (π , η), vector (ρ , ω) and scalar σ exchanges are considered [4, 7, 16, 17]. The existence of such molecular states is also confirmed by the calculation in the constituent quark model with the meson-exchange mechanism at the quark level [6, 8].

Up to now, these hidden-charm pentaquarks were only observed in the Λ_b decay at LHCb. Production of the pentaquarks in other ways is very helpful to obtain the definite evidence for their nature as genuine states. Before LHCb's observation of $P_c(4450)$ and $P_c(4380)$, the production of hidden-charm pentaquark in the $p\bar{p} \rightarrow p\bar{p}J/\psi$ process was proposed in the article in which the hidden-charm pentaquark was predicted [18]. The photoproduction of the hidden-charm pentaquark was first suggested to be applied at Jefferson Laboratory in Ref. [19]. After the LHCb experiment, more works about the production of the $P_c(4450)$ and $P_c(4380)$ appeared [20–23]. In particular an experimental proposal to search for the $P_c(4450)$ in J/ψ photoproduction was put forward to be performed in Hall C at Jefferson Lab [24]. At present, there are already some experimental data [25–27] for the reaction $\gamma p \rightarrow J/\psi p$. One notes that there exist large uncertainties in existing experimental data [25–27] in the near-threshold energy region where the P_c states live. The high-luminosity detectors at Jefferson Laboratory will pro-

* xywang01@outlook.com

† xchen@impcas.ac.cn

‡ Corresponding author : junhe@njnu.edu.cn

duce high-precision data in future experiments. One can expect these experiments to provide an opportunity to study the hidden-charm pentaquarks in photoproduction.

In the new LHCb results, the $P_c(4450)$ splits into two states, $P_c(4440)$ and $P_c(4457)$. These two states are quite narrower than the $P_c(4450)$, which will affect previous predictions about the photoproduction of the P_c states. Moreover, a new pentaquark $P_c(4312)$ was observed. Hence, it is interesting to restudy the photoproduction of the pentaquarks based on the new LHCb results [3]. In this paper, within the framework of an effective Lagrangian approach, the photoproduction of three P_c states via reaction $\gamma p \rightarrow J/\psi p$ is investigated. The t -channel Pomeron exchange diffractive process is considered as the main background.

This paper is organized as follows. After the Introduction, we present the formalism including Lagrangians and amplitudes for the $\gamma p \rightarrow J/\psi p$ process in Sec. II. The numerical results of the cross section follow in Sec. III. Finally, the paper ends with a brief summary.

II. FORMALISM

The basic tree-level Feynman diagrams of the reactions $\gamma p \rightarrow J/\psi p$ are illustrated in Fig. 1 in which the pentaquark P_c candidates are produced through s and u channel. The background contribution is mainly from the t -channel Pomeron exchange, as depicted in Fig. 1(c). Considering the off-shell effect of the intermediate P_c states, the u -channel contribution will be neglected in our calculation.

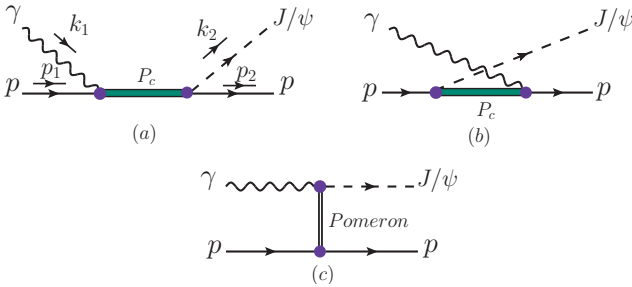


FIG. 1. Feynman diagrams for the reaction $\gamma p \rightarrow J/\psi p$.

A. Lagrangians for P_c photoproduction

At present, the spin-parity quantum numbers of these P_c states were not determined experimentally. In this work, the theoretical prediction of $P_c(4312)$ with $J^P = 1/2^-$, $P_c(4440)$ with $J^P = 1/2^-$ and $P_c(4457)$ with $J^P = 3/2^-$ are taken in our calculation as suggested in Refs. [4, 6–8, 10, 13]. For describing the P_c photoproduction process, Lagrangians are needed [23, 28–31],

$$\mathcal{L}_{\gamma NP_c}^{1/2^-} = \frac{eh}{2m_N} \bar{N} \sigma_{\mu\nu} \partial^\nu A^\mu P_c + \text{H.c.}, \quad (2)$$

$$\mathcal{L}_{P_c\psi N}^{1/2^-} = g_{P_c\psi N}^{1/2^-} \bar{N} \gamma_5 \gamma_\mu P_c \psi^\mu + \text{H.c.}, \quad (3)$$

$$\mathcal{L}_{\gamma NP_c}^{3/2^-} = e \left(\frac{ih_1}{2m_N} \bar{N} \gamma^\nu - \frac{h_2}{(2m_N)^2} \partial^\nu \bar{N} \right) \times F_{\mu\nu} P_c^\mu + \text{H.c.}, \quad (4)$$

$$\mathcal{L}_{P_c\psi N}^{3/2^-} = \frac{-ig_{P_c\psi N}^{3/2^-}}{2m_N} \bar{N} \gamma_\nu \psi^{\mu\nu} P_{c\mu} - \frac{g_2}{(2m_N)^2} \partial_\nu \bar{N} \psi^{\mu\nu} P_{c\mu} + \frac{g_2}{(2m_N)^2} \bar{N} \partial_\nu \psi^{\mu\nu} P_{c\mu} + \text{H.c.}, \quad (5)$$

where $F_{\mu\nu} = \partial_\mu A_\nu - \partial_\nu A_\mu$ and N , A , P_c , and ψ are the nucleon, photon, P_c state, and J/ψ meson fields, respectively.

Since the momenta of the final states $J/\psi N$ are fairly small compared with the nucleon mass, the higher partial wave terms in Eqs. (4) and (5) will be neglected in the following, calculated as done in Ref. [23].

The value of $g_{P_c\psi N}^{1/2^-}$ and $g_{P_c\psi N}^{3/2^-}$ can be determined from the decay width

$$\Gamma_{P_c \rightarrow \psi N}^{1/2^-} = \frac{|\vec{p}_\psi^{\text{c.m.}}|}{16\pi m_{P_c}^2} \left| \mathcal{M}_{P_c \rightarrow \psi N}^{1/2^-} \right|^2, \quad (6)$$

$$\Gamma_{P_c \rightarrow \psi N}^{3/2^-} = \frac{|\vec{p}_\psi^{\text{c.m.}}|}{32\pi m_{P_c}^2} \left| \mathcal{M}_{P_c \rightarrow \psi N}^{3/2^-} \right|^2, \quad (7)$$

with

$$|\vec{p}_\psi^{\text{c.m.}}| = \frac{\lambda(m_{P_c}^2, m_\psi^2, m_N^2)}{2m_{P_c}}, \quad (8)$$

where λ is the Källén function with $\lambda(x, y, z) \equiv \sqrt{(x-y-z)^2 - 4yz}$. The m_{P_c} , m_ψ , and m_N are the masses of P_c , J/ψ , and the nucleon. $\mathcal{M}_{P_c \rightarrow \psi N}^{1/2^-}$ and $\mathcal{M}_{P_c \rightarrow \psi N}^{3/2^-}$ are the decay amplitudes.

For the electromagnetic (EM) coupling eh related to the γNP_c vertex, its value can be obtained from the strong coupling constant $g_{P_c\psi N}$ within the vector meson dominance (VMD) mechanism [32–34]. In the frame of the VMD mechanism, the EM coupling constants eh and eh_1 are related to the coupling constants $g_{P_c\psi N}^{1/2^-}$ and $g_{P_c\psi N}^{3/2^-}$ as

$$eh = g_{P_c\psi N}^{1/2^-} \frac{e}{f_\psi} \frac{2m_N}{(m_{P_c}^2 - m_N^2)m_\psi} \times \sqrt{m_\psi^2(m_N^2 + 4m_N m_{P_c} + m_{P_c}^2) + (m_{P_c}^2 - m_N^2)^2}, \quad (9)$$

$$eh_1 = g_{P_c\psi N}^{3/2^-} \frac{e}{f_\psi} \frac{2m_N(m_N + m_{P_c})}{(m_{P_c}^2 - m_N^2)m_\psi} \times \sqrt{\frac{6m_\psi^2 m_{P_c}^2 + m_N^4 - 2m_N^2 m_{P_c}^2 + m_{P_c}^4}{3m_{P_c}^2 + m_N^2}}. \quad (10)$$

The Lagrangian depicting the coupling of the meson J/ψ with a photon reads as

$$\mathcal{L}_{J/\psi\gamma} = -\frac{em_\psi^2}{f_\psi} V_\mu A^\mu, \quad (11)$$

where f_ψ is the J/ψ decay constant. Thus one gets the expression for the $J/\psi \rightarrow e^+e^-$ decay,

$$\Gamma_{J/\psi \rightarrow e^+e^-} = \left(\frac{e}{f_\psi}\right)^2 \frac{8\alpha |\vec{p}_e^{\text{c.m.}}|^3}{3m_\psi^2}, \quad (12)$$

where $\vec{p}_e^{\text{c.m.}}$ denotes the 3-momentum of an electron in the rest frame of the J/ψ meson. The $\alpha = e^2/4\hbar c = 1/137$ is the electromagnetic fine structure constant. With the partial decay width of $J/\psi \rightarrow e^+e^-$ [1],

$$\Gamma_{J/\psi \rightarrow e^+e^-} \simeq 5.547 \text{ keV}, \quad (13)$$

one gets $e/f_\psi \simeq 0.027$.

Finally, one obtains the EM couplings related to the γNP_c vertices and coupling constants $g_{P_c\psi N}$ from partial decay widths $\Gamma_{P_c \rightarrow \psi N}$ with different J^P assignments of the P_c states. The obtained coupling constants are listed in Tables I and II by assuming that the $J/\psi p$ channel accounts for 3% and 10% of total widths of the P_c states, respectively.

TABLE I. The values of coupling constants by assuming the $J/\psi p$ channel accounts for 3% of total widths of the P_c states.

States	$g_{P_c\psi N}$	eh or eh_1
$P_c(4312) (J^P = \frac{1}{2}^-)$	0.06	0.0014
$P_c(4440) (J^P = \frac{1}{2}^-)$	0.08	0.0018
$P_c(4457) (J^P = \frac{3}{2}^-)$	0.036	0.0008

TABLE II. The values of coupling constants by assuming the $J/\psi p$ channel accounts for 10% of total widths of the P_c states.

States	$g_{P_c\psi N}$	eh or eh_1
$P_c(4312) (J^P = \frac{1}{2}^-)$	0.11	0.0026
$P_c(4440) (J^P = \frac{1}{2}^-)$	0.14	0.0032
$P_c(4457) (J^P = \frac{3}{2}^-)$	0.07	0.0016

B. Pomeron exchange

Since the Pomeron can mediate the long-range interaction between a confined quark and a nucleon [35–38], the t -channel Pomeron exchange [as described in Fig. 1(c)] is considered the main background contribution to the $P_c(4312)$ photoproduction process. The Pomeron exchange is expressed in terms of the quark loop coupling in the vertices of $\mathbb{P}NN$ and $\gamma\mathbb{P}\psi$. The Pomeron-nucleon coupling is written as [35–38]

$$\mathcal{F}_\rho(t) = \frac{3\beta_0(4m_N^2 - 2.8t)}{(4m_N^2 - t)(1 - t/0.7)^2} \gamma_\rho = F(t)\gamma_\rho, \quad (14)$$

where $t = q_p^2$ is the exchanged Pomeron momentum squared. $\beta_0^2 = 4 \text{ GeV}^2$ stands for the coupling constant between a single Pomeron and a light constituent quark.

For the $\gamma\mathbb{P}\psi$ vertex, we have

$$V_{\gamma\mathbb{P}\psi} = \frac{2\beta_c \times 4\mu_0^2}{(m_\psi^2 - t)(2\mu_0^2 + m_\psi^2 - t)} T_{\rho,\mu\nu} \epsilon_\psi^\nu \epsilon_\gamma^\mu \mathbb{P}^\rho, \quad (15)$$

with

$$T^{\rho,\mu\nu} = (k_1 + k_2)^\rho g^{\mu\nu} - 2k_1^\nu g^{\rho\mu}$$

where $\beta_c^2 = 0.8 \text{ GeV}^2$ is the effective coupling constant between a Pomeron and a charm quark within the J/ψ meson [35, 39], while $\mu_0 = 1.2 \text{ GeV}^2$ denotes a cutoff parameter in the form factor of the Pomeron [35–38].

C. Amplitudes

According to the above Lagrangians, the scattering amplitude of the reaction $\gamma p \rightarrow J/\psi p$ can be written as

$$-i\mathcal{M} = \epsilon_\psi^\nu(k_2) \bar{u}(p_2) \mathcal{A}_{\mu\nu}^i u(p_1) \epsilon_\gamma^\mu(k_1), \quad (16)$$

where u is the Dirac spinor of nucleon, and ϵ_ψ^ν and ϵ_γ^μ are the polarization vector of J/ψ meson and photon, respectively.

The reduced amplitudes $\mathcal{A}_{\mu\nu}^i$ for the s channel with each J^P assignment of P_c state and the t channel read

$$\mathcal{A}_{\mu\nu}^{s(1/2^-)} = \frac{eh}{2m_N} g_{P_c\psi N} \mathcal{F}(q^2) \gamma_5 \gamma_\nu \frac{(\not{q} + m_{P_c})}{s - m_{P_c}^2 + im_{P_c} \Gamma_{P_c}} \times \gamma_\mu \not{k}_1, \quad (17)$$

$$\mathcal{A}_{\mu\nu}^{s(3/2^-)} = \frac{eh_1}{2m_N} \frac{g_{P_c\psi N}}{2m_N} \mathcal{F}(q^2) \gamma_\sigma (k_2^\beta g^{\nu\sigma} - k_2^\sigma g^{\nu\beta}) \times \frac{(\not{q} + m_{P_c})}{s - m_{P_c}^2 + im_{P_c} \Gamma_{P_c}} \Delta_{\beta\alpha} \gamma_\delta (k_1^\alpha g^{\mu\delta} - k_1^\delta g^{\alpha\mu}), \quad (18)$$

$$\mathcal{A}_{\mu\nu}^t = 8\beta_c \mu_0^2 \frac{\mathcal{F}_\rho(t) G_P(s, t)}{(m_\psi^2 - t)(2\mu_0^2 + m_\psi^2 - t)} T^{\rho,\mu\nu}, \quad (19)$$

with

$$\Delta_{\beta\alpha} = -g_{\beta\alpha} + \frac{1}{3} \gamma^\beta \gamma^\alpha + \frac{1}{3m_{P_c}} (\gamma^\beta q^\alpha - \gamma^\alpha q^\beta) + \frac{2}{3m_{P_c}^2} q^\beta q^\alpha, \quad (20)$$

$$G_P(s, t) = -i(\eta' s) \eta^{(t)-1} \quad (21)$$

where $\eta(t) = 1 + \epsilon + \eta' t$ is the Pomeron Regge trajectory, while the concrete values $\epsilon = 0.08$ and $\eta' = 0.25 \text{ GeV}^{-2}$ are adopted [35–38]. Moreover, $s = (k_1 + p_1)^2$ and $t = (k_1 - k_2)^2$ are the Mandelstam variables.

For the s channel with an intermediate P_c state, one adopts a general form factor to describe the size of hadrons as [23, 40, 41]

$$\mathcal{F}(q^2) = \frac{\Lambda^4}{\Lambda^4 + (q^2 - m_{P_c}^2)^2}, \quad (22)$$

where q and m_{P_c} are the 4-momentum and mass of the exchanged P_c state, respectively. For the heavier hadron production, the typical cutoff value $\Lambda = 0.5$ GeV will be taken as used in Refs. [23, 30].

III. NUMERICAL RESULTS

With the preparation in the previous section, the cross section of the reaction $\gamma p \rightarrow J/\psi p$ can be calculated. The differential cross section in the c.m. frame is written as

$$\frac{d\sigma}{d\cos\theta} = \frac{1}{32\pi s} \frac{|\vec{k}_2^{\text{c.m.}}|}{|\vec{k}_1^{\text{c.m.}}|} \left(\frac{1}{4} \sum_{\lambda} |\mathcal{M}|^2 \right), \quad (23)$$

where $s = (k_1 + p_1)^2$ and θ denotes the angle of the outgoing J/ψ meson relative to photon beam direction in the c.m. frame. $\vec{k}_1^{\text{c.m.}}$ and $\vec{k}_2^{\text{c.m.}}$ are the 3-momenta of the initial photon beam and final J/ψ meson, respectively.

In Fig. 2, we present the total cross section for the reaction $\gamma p \rightarrow J/\psi p$ by assuming a branching ratio $Br[P_c \rightarrow J/\psi p] \simeq 3\%$ from threshold to 24 GeV of the photon beam energy. It is found that the line shape of the total cross section including both P_c and Pomeron contributions goes up very rapidly. The experimental data of the $\gamma p \rightarrow J/\psi p$ process seem to be quite consistent with the total cross section. Moreover, the value of the total cross section becomes larger and larger with the increase of the beam energy up to 24 GeV. The monotonically increasing behavior should be caused by the t -channel Pomeron exchange. Obviously, the contribution from the Pomeron diffractive process is responsible for explaining the experimental data points at high energies. The $P_c(4312)$ exhibits itself as an independent peak, while the $P_c(4440)$ and $P_c(4457)$ are very close to each other with the masses observed at LHCb.

To show the results for three pentaquarks more clearly, in Fig. 3, we give the same results as Fig. 2 but with a reduced energy range. The peak for the $P_c(4312)$ still stands independently. The $P_c(4450)$ and $P_c(4457)$ can be distinguished in the reduced energy region. The results suggest that the $P_c(4312)$ can be observed within a bin of 0.1 GeV. For the two higher pentaquarks, $P_c(4440)$ and $P_c(4457)$, the mass difference is only about 17 MeV, which is comparable to the widths of these two pentaquarks. Hence, if we adopt a large bin, such as 0.1 GeV, the $P_c(4440)$ and $P_c(4457)$ will exhibit as one resonance. The dip in the two-peak structure of these two states will disappear because the cross section should be averaged in a bin. To distinguish these two close states, we should choose several energy points between two peaks of $P_c(4440)$ and $P_c(4457)$, which requires a bin at least at an order of 10 MeV based on our calculation. Our results suggest that the total cross section is of order 1 nb. Hence, by assuming a branching ratio $Br[P_c \rightarrow J/\psi p] \simeq 3\%$, to observe the $P_c(4312)$, the experimental precision should be 1nb/0.1 GeV. However, to observe the two-peak structure from the $P_c(4440)$ and $P_c(4457)$, higher precision, 0.1nb/10 MeV, is required based on our results.

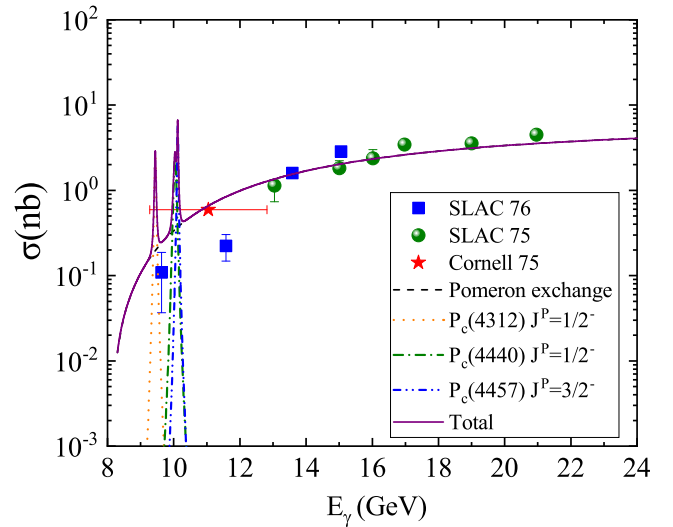


FIG. 2. Total cross section for the reaction $\gamma p \rightarrow J/\psi p$ by assuming branching ratio $Br[P_c \rightarrow J/\psi p] \simeq 3\%$. The black dashed, orange dotted, green dot-dashed, blue dash-double dotted, and violet solid lines are for the Pomeron exchange, $P_c(4312)$, $P_c(4440)$, $P_c(4457)$, and total contributions, respectively. The experimental data are from Refs. [25–27].

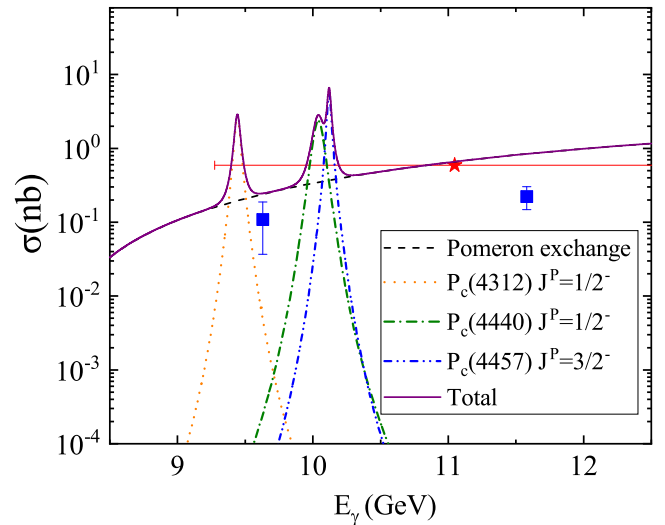


FIG. 3. Same as Fig. 2 except that the energy range is reduced.

In Fig. 4, we show the obtained total cross section of the $\gamma p \rightarrow J/\psi p$ process as a function of the photon beam energy, where the result are calculated by assuming $Br[P_c \rightarrow J/\psi p] \simeq 10\%$. It can be seen that the total cross section exhibits three peaks near the threshold. In the near-threshold energy region, the contributions from the s -channel P_c -state exchanges are at least an order of magnitude higher than the cross section from the background from the Pomeron exchange, which indicates that the signal can be clearly distinguished from the background. Thus, the range $E_\gamma \simeq 9.4 - 10.5$ GeV should be

the best energy window of searching for these P_c states via the photoinduced process.

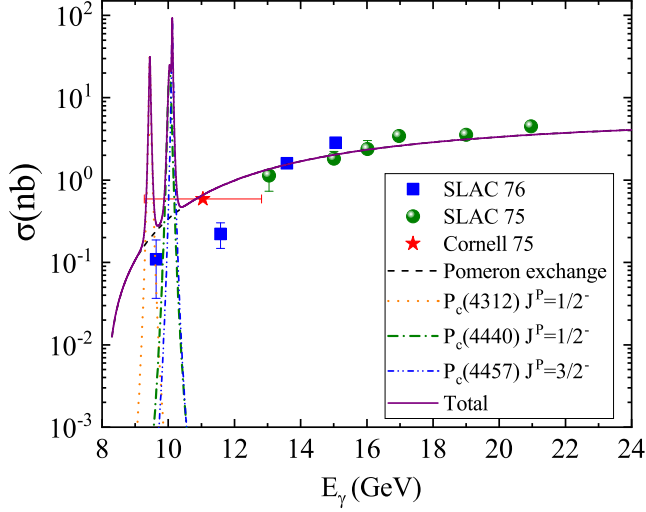


FIG. 4. Same as Fig. 2 except assuming a branching ratio $Br[P_c \rightarrow J/\psi p] \approx 10\%$.

The differential cross sections corresponding to branching ratios $Br[P_c \rightarrow J/\psi p] \approx 3\%$ and 10% are illustrated in Figs. 5 and 6, respectively. One notices that the differential cross sections are enhanced in the forward direction because of the strong Pomeron diffractive contribution in the t channel. In the regions of the P_c states, i.e., $E_\gamma = 9.4, 10.0,$ and 10.1 GeV, the effects of the P_c states are obvious, which makes the curve of differential cross sections tend to be flat. The shape of the differential cross section from the pentaquark is relevant to the orbital angular momentum between the final and initial particles. Under the assignment of the spin parities of the pentaquarks in the current work, the pentaquarks can couple to both the final $J/\psi p$ and initial γp in the S wave and the higher partial waves are neglected because the momentum between the final $J/\psi p$ is fairly small. The flatness reflects such assignment of the spin parities. The nondiffractive effects at off-forward angles in the range of near-threshold energies can be measured by future experiments, which will help us to clarify the role of P_c states in the reaction $\gamma p \rightarrow J/\psi p$.

We will now discuss the polarization observables, which can provide crucial information on the helicity amplitudes and spin structure of a process [42]. To define the polarization observables, the reaction takes place in the $x-z$ plane. The photon beam asymmetry Σ_γ is defined as

$$\Sigma_\gamma = \frac{d\sigma(\epsilon_\perp) - d\sigma(\epsilon_\parallel)}{d\sigma(\epsilon_\perp) + d\sigma(\epsilon_\parallel)}, \quad (24)$$

where \parallel and \perp denote the linear polarizations of the photon along the direction of the x and y axes, respectively. Figure 7 depicts the numerical results of the photon beam asymmetries Σ_γ for the reaction $\gamma p \rightarrow J/\psi p$ at different beam energies. One notices that the contributions from the P_c states have a greater impact on the polarization observation Σ_γ near

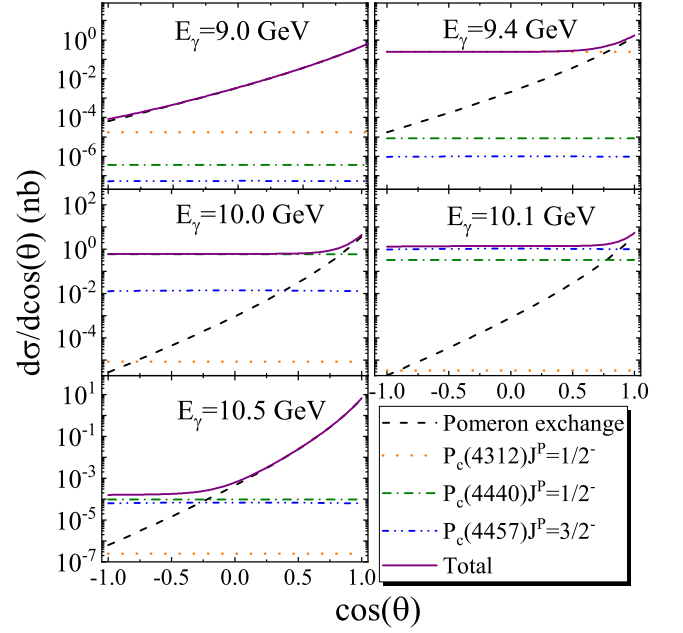


FIG. 5. The differential cross section $d\sigma/d\cos\theta$ of the $\gamma p \rightarrow J/\psi p$ process as a function of $\cos\theta$ at beam energies $E_\gamma = 9.0, 9.4, 10.0, 10.1,$ and 10.5 GeV. The coupling constants are extracted by assuming branching ratio $Br[P_c \rightarrow J/\psi p] \approx 3\%$. The black dashed, orange dotted, green dot-dashed, blue dash-double dotted, and violet solid lines are for the Pomeron exchange, $P_c(4312)J^P=1/2^-$, $P_c(4440)J^P=1/2^-$, $P_c(4457)J^P=3/2^-$, and total contributions, respectively.

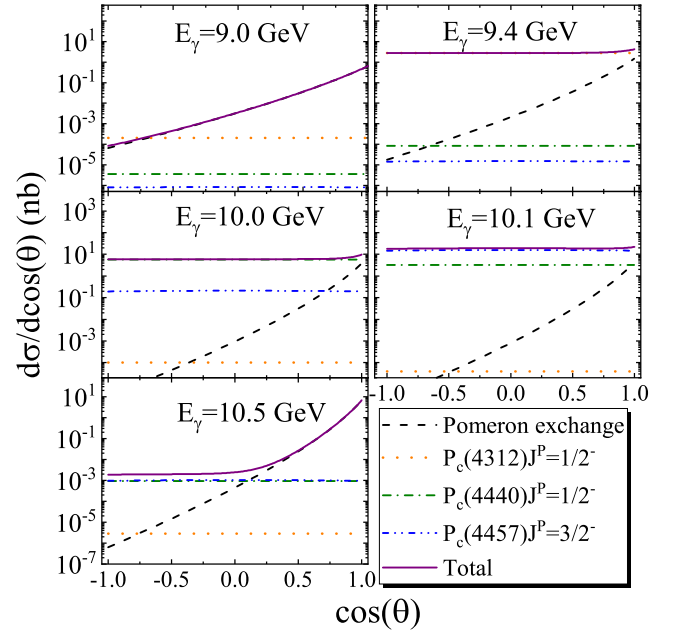


FIG. 6. Same as Fig. 4 except by assuming branching ratio $Br[P_c \rightarrow J/\psi p] \approx 10\%$.

the threshold. Thus, the measurement of the beam asymmetry will help us clarify the roles of these P_c states in the $\gamma p \rightarrow J/\psi p$ process.

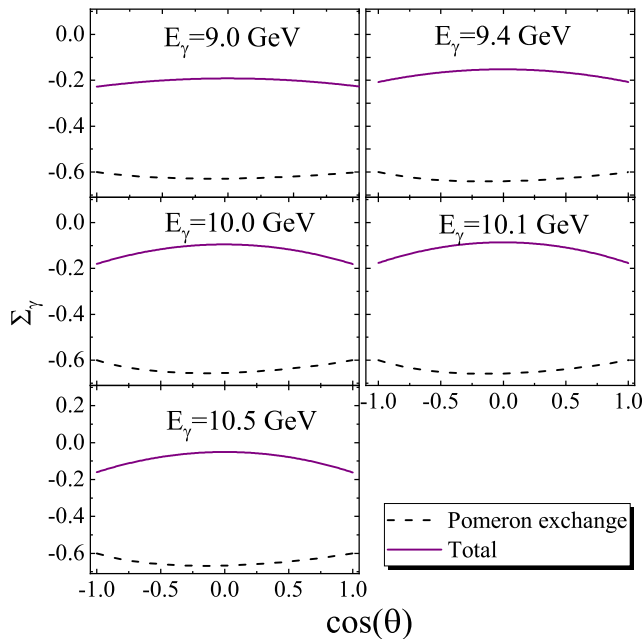


FIG. 7. The photon beam asymmetries Σ_γ for the reaction $\gamma p \rightarrow J/\psi p$ of $E_\gamma = 9.0 - 10.5$ GeV. The violet solid curves represent the total results including the P_c states, whereas the black dashed lines only show the result of Pomeron exchange.

IV. SUMMARY AND DISCUSSION

Within the frame of the effective Lagrangian approach and the VMD model, the production of pentaquark states $P_c(4312)$, $P_c(4440)$, and $P_c(4457)$ via the s channel in the reaction $\gamma p \rightarrow J/\psi p$ is investigated. Moreover, the t -channel Pomeron exchange is also studied, and is regarded as the background for the photoproduction of the P_c states. The numerical results show that existing experimental data for the $\gamma p \rightarrow J/\psi p$ process are consistent with the present result by assuming the branching ratio $Br[P_c \rightarrow J/\psi p] \approx 3\%$. If the branching ratio of P_c decay to $J/\psi p$ is small, these pentaquark P_c states may have stronger couplings to other channels, i.e., $\Sigma_c \bar{D}$, $\Sigma_c \bar{D}^*$ etc. A precision of 0.1 nb/10 MeV is required to distinguish the $P_c(4440)$ and $P_c(4457)$. The total cross section of the $\gamma p \rightarrow J/\psi p$ process is also calculated by taking $Br[P_c \rightarrow J/\psi p] \approx 10\%$. The contribution of these P_c states

makes several distinct peaks, which are at least 1 order of magnitude larger than the background cross section, appear in the cross section at the near-threshold energy region. Hence, if $Br[P_c \rightarrow J/\psi p] \approx 3\%$ is in line with the actual situation, it is feasible to search for these pentaquark P_c states via the reaction $\gamma p \rightarrow J/\psi p$ with the precision suggested above, in which the signal can be clearly distinguished from the background. If the physical branching ratio is larger, lower precision will be required in experiment.

The differential cross sections for the reaction $\gamma p \rightarrow J/\psi p$ are also calculated. One notices that the cross section of the t -channel Pomeron exchange is sensitive to the θ angle and gives a considerable contribution at forward angles. The contributions of the P_c states are mainly concentrated near the threshold energy region and make the differential cross section relatively flat, which is consistent with our choice of the spin parities of the pentaquarks. The polarization observable Σ_γ is also calculated, and the results suggest that the P_c states have large effects on this observable.

To deepen the understanding of these pentaquark P_c states, an experimental study of the P_c states via the photo-induced process is strongly suggested. The photon beams can be provided at JLab[24, 43] and COMPASS [44]. The center-of-mass energy 4.5 GeV corresponds to a laboratory photon energy of 10.5 GeV, which is well within the capabilities of the GlueX and CLAS12 detectors at JLab [24, 43, 45]. The calculations of the current work suggest that it is promising to do such experiments at existing facilities. The expected high-precision data at the threshold energy region will not only be helpful in clarifying the role of the pentaquark states $P_c(4312)$, $P_c(4440)$, and $P_c(4457)$ in reaction $\gamma p \rightarrow J/\psi p$ but also will help provide important information for better understanding the nature of these P_c states.

V. ACKNOWLEDGMENTS

This project is supported by the National Natural Science Foundation of China under Grants No. 11705076 and No. 11675228. We acknowledge the Natural Science Foundation of Gansu province under Grant No. 17JR5RA113. This work is partly supported by the HongLiu Support Funds for Excellent Youth Talents of Lanzhou University of Technology.

-
- [1] M. Tanabashi *et al.* [ParticleDataGroup], “Review of Particle Physics,” *Phys. Rev. D* **98**, 030001 (2018).
 - [2] R. Aaij *et al.* [LHCb Collaboration], “Observation of $J/\psi p$ Resonances Consistent with Pentaquark States in $\Lambda_b^0 \rightarrow J/\psi K^- p$ Decays,” *Phys. Rev. Lett.* **115**, 072001 (2015).
 - [3] R. Aaij *et al.* [LHCb Collaboration], “Observation of a narrow pentaquark state, $P_c(4312)^+$, and of two-peak structure of the $P_c(4450)^+$,” arXiv:1904.03947 [hep-ex].
 - [4] R. Chen, Z. F. Sun, X. Liu and S. L. Zhu, “Strong LHCb evidence supporting the existence of the hidden-charm molecular pentaquarks,” arXiv:1903.11013 [hep-ph].
 - [5] H. X. Chen, W. Chen and S. L. Zhu, “Possible interpretations of the $P_c(4312)$, $P_c(4440)$, and $P_c(4457)$,” arXiv:1903.11001 [hep-ph].
 - [6] M. Z. Liu, Y. W. Pan, F. Z. Peng, M. Sánchez Sánchez, L. S. Geng, A. Hosaka and M. Pavon Valderrama, “Emergence of a complete heavy-quark spin symmetry multiplet: seven molecular pentaquarks in light of the latest LHCb analysis,” arXiv:1903.11560 [hep-ph].
 - [7] J. He, “Study of $P_c(4457)$, $P_c(4440)$, and $P_c(4312)$ in a quasipotential Bethe-Salpeter equation approach,” *Eur. Phys. J. C* **79**, 393 (2019).

- [8] H. Huang, J. He and J. Ping, “Looking for the hidden-charm pentaquark resonances in $J/\psi p$ scattering,” arXiv:1904.00221 [hep-ph].
- [9] A. Ali and A. Y. Parkhomenko, “Interpretation of the Narrow $J/\psi p$ Peaks in $\Lambda_b \rightarrow J/\psi p K^-$ Decay in the Compact Diquark Model,” Phys. Lett. B, **793**, 365 (2019).
- [10] C. J. Xiao, Y. Huang, Y. B. Dong, L. S. Geng and D. Y. Chen, “Partial decay widths of $P_c(4312)$, $P_c(4440)$, and $P_c(4457)$ into $J/\psi p$ in a molecular scenario,” arXiv:1904.00872 [hep-ph].
- [11] Y. Shimizu, Y. Yamaguchi and M. Harada, “Heavy quark spin multiplet structure of $P_c(4312)$, $P_c(4440)$, and $P_c(4457)$,” arXiv:1904.00587 [hep-ph].
- [12] Z. H. Guo and J. A. Oller, “Anatomy of the newly observed hidden-charm pentaquark states: $P_c(4312)$, $P_c(4440)$ and $P_c(4457)$,” Phys. Lett. B **793**, 144 (2019)
- [13] C. W. Xiao, J. Nieves and E. Oset, “Heavy quark spin symmetric molecular states from $\bar{D}^{(*)}\Sigma_c^{(*)}$ and other coupled channels in the light of the recent LHCb pentaquarks,” arXiv:1904.01296 [hep-ph].
- [14] F. K. Guo, H. J. Jing, U. G. Meißner and S. Sakai, “Isospin breaking decays as a diagnosis of the hadronic molecular structure of the $P_c(4457)$,” Phys. Rev. D **99**, 091501 (2019).
- [15] X. Cao and J. p. Dai, “Pentaquark photoproduction confronting with new LHCb observation,” arXiv:1904.06015 [hep-ph].
- [16] J. He, “ $\bar{D}\Sigma_c^*$ and $\bar{D}^*\Sigma_c$ interactions and the LHCb hidden-charmed pentaquarks,” Phys. Lett. B **753**, 547 (2016)
- [17] Z. C. Yang, Z. F. Sun, J. He, X. Liu and S. L. Zhu, “The possible hidden-charm molecular baryons composed of anti-charmed meson and charmed baryon,” Chin. Phys. C **36**, 6 (2012)
- [18] J. J. Wu, R. Molina, E. Oset and B. S. Zou, “Prediction of narrow N^* and Λ^* resonances with hidden charm above 4 GeV,” Phys. Rev. Lett. **105**, 232001 (2010)
- [19] Y. Huang, J. He, H. F. Zhang and X. R. Chen, “Discovery potential of hidden charm baryon resonances via photoproduction,” J. Phys. G **41**, 115004 (2014).
- [20] Q. F. Lü, X. Y. Wang, J. J. Xie, X. R. Chen and Y. B. Dong, “Neutral hidden charm pentaquark states $P_c^0(4380)$ and $P_c^0(4450)$ in $\pi^- p \rightarrow J/\psi n$ reaction,” Phys. Rev. D **93**, 034009 (2016).
- [21] E. J. Garzon and J. J. Xie, “Effects of a N_{cc}^* resonance with hidden charm in the $\pi^- p \rightarrow D^- \Sigma_c^+$ reaction near threshold,” Phys. Rev. C **92**, 035201 (2015).
- [22] M. Karliner and J. L. Rosner, “Photoproduction of Exotic Baryon Resonances,” Phys. Lett. B **752**, 329 (2016).
- [23] Q. Wang, X. H. Liu and Q. Zhao, “Photoproduction of hidden charm pentaquark states $P_c^+(4380)$ and $P_c^+(4450)$,” Phys. Rev. D **92**, 034022 (2015).
- [24] Z. E. Meiziani *et al.*, “A Search for the LHCb Charmed ‘Pentaquark’ using Photo-Production of J/ψ at Threshold in Hall C at Jefferson Lab,” arXiv:1609.00676 [hep-ex].
- [25] B. Gittelman *et al.*, “Photoproduction of the psi (3100) Meson at 11-GeV,” Phys. Rev. Lett. **35**, 1616 (1975).
- [26] U. Camerini *et al.*, “Photoproduction of the psi Particles,” Phys. Rev. Lett. **35**, 483 (1975).
- [27] Robert L. Anderson, “Excess Muons and New Results in ψ Photoproduction,” Microfiche at Fermilab, (1976).
- [28] X. Y. Wang and J. He, “ $K^{*0}\Lambda$ photoproduction off a neutron,” Phys. Rev. C **93**, 035202 (2016).
- [29] X. Y. Wang, J. He and H. Haberzettl, “Analysis of recent CLAS data on $\Sigma^*(1385)$ photoproduction off a neutron target,” Phys. Rev. C **93**, 045204 (2016).
- [30] S. H. Kim, S. i. Nam, Y. Oh and H. C. Kim, “Contribution of higher nucleon resonances to $K^*\Lambda$ photoproduction,” Phys. Rev. D **84**, 114023 (2011).
- [31] Y. Oh, C. M. Ko and K. Nakayama, “Nucleon and Delta resonances in K Sigma(1385) photoproduction from nucleons,” Phys. Rev. C **77**, 045204 (2008).
- [32] T. H. Bauer, *et al.*, Rev. Mod. Phys. **50**, 261 (1978); 51, 407(E) (1979).
- [33] T. Bauer and D. R. Yennie, Phys. Lett. B **60**, 165 (1976).
- [34] T. Bauer and D. R. Yennie, Phys. Lett. B **60**, 169 (1976).
- [35] X. H. Liu, Q. Zhao and F. E. Close, “Search for tetraquark candidate Z(4430) in meson photoproduction,” Phys. Rev. D **77**, 094005 (2008).
- [36] X. Y. Wang, X. R. Chen and A. Guskov, “Photoproduction of the charged charmoniumlike $Z_c^+(4200)$,” Phys. Rev. D **92**, 094017 (2015).
- [37] A. Donnachie and P. V. Landshoff, “Exclusive rho Production in Deep Inelastic Scattering,” Phys. Lett. B **185**, 403 (1987).
- [38] M. A. Pichowsky and T. S. H. Lee, “Pomeron exchange and exclusive electroproduction of rho mesons in QCD,” Phys. Lett. B **379**, 1 (1996).
- [39] J. M. Laget and R. Mendez-Galain, “Exclusive photoproduction and electroproduction of vector mesons at large momentum transfer,” Nucl. Phys. A **581**, 397 (1995).
- [40] X. Y. Wang and J. He, “Investigation of pion-induced $f_1(1285)$ production off a nucleon target within an interpolating Reggeized approach,” Phys. Rev. D **96**, 034017 (2017).
- [41] X. Y. Wang and X. R. Chen, “Production of the superheavy baryon $\Lambda_{cc}^+(4209)$ in kaon-induced reaction,” Eur. Phys. J. A **51**, 85 (2015).
- [42] C. G. Fasano, F. Tabakin and B. Saghai, “Spin observables at threshold for meson photoproduction,” Phys. Rev. C **46**, 2430 (1992).
- [43] A. Austregesilo [GlueX Collaboration], “Light-Meson Spectroscopy at GlueX,” Int. J. Mod. Phys. Conf. Ser. **46**, 1860029 (2018).
- [44] F. Nerling [COMPASS Collaboration], “Hadron Spectroscopy with COMPASS: Newest Results,” EPJ Web Conf. **37**, 01016 (2012).
- [45] S. Kumano, “Spin Physics at J-PARC,” Int. J. Mod. Phys. Conf. Ser. **40**, 1660009 (2016).